

Development and Optimization of a Tubular Linear Synchronous Motor Considering Various Skewing Methods and Eddy Current Losses

A. D. P. Juliani, M. Leßmann, D. P. Gonzaga, K. Hameyer

Abstract – Electromagnetic force with minimum ripple is desirable in many applications. Therefore, the cogging force must be analyzed and solutions for its reduction must be worked out. This paper investigates two possible ways of skewing the magnets of a permanent magnet excited tubular linear synchronous motor to reduce the cogging force. In bioengineering applications, specially upper limb prostheses, minimizing losses is also an issue to prevent tissue overheating, which can lead to hemolysis and thrombogenicity. Hence, the eddy current and hysteresis losses are investigated and related to the ohmic losses.

Index Terms – Eddy Current Losses, Permanent Magnet Excited Synchronous Machine, Skewed Magnets, Tubular Linear Motor, Upper Limb Prostheses.

I. INTRODUCTION

Permanent magnets offer many advantages over electromagnetic excitation in electric machines, such as higher efficiency, higher force or/and output power per volume, better dynamic performance, simplified construction and maintenance [1]. However, the attraction between magnets and stator teeth causes cogging forces.

In applications that require an accurate computation of electromagnetic forces, the minimization of cogging force is an important design issue. Here are particularly concerned all applications where electric motors are responsible for producing accurate movements, like among others those applied to prostheses, orthoses, or surgery robots.

In this paper, a permanent magnet excited tubular linear synchronous motor is used to actuate an upper limb prostheses. Fig. 1 shows the mechanism of a finger, whose joints are constituted by pulleys and springs. The electrical linear motor is responsible for the abduction movement, whereas torsion springs realize the extension.

In bioengineering, especially the transmission of heat towards the surrounding tissue is a challenging problem. Tissue temperatures above 42°C increase the risk of hemolysis and thrombogenicity [2]. Hence, optimal actuator efficiencies are required to minimize the risk of blood disease. This favours permanent magnet machines, which work with no excitation losses. Other losses are the ohmic losses in the stator coils, the eddy current losses in all electric conducting parts as well as the hysteresis losses in ferromagnetic materials.

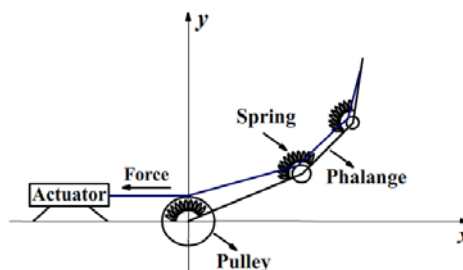


Fig. 1. Mechanical mechanism of a finger adapted from [6].

This paper analyses the cogging force of the permanent magnet excited tubular linear synchronous motor applied to upper limb prostheses. For minimization of cogging force, two skewing approaches of the rotor magnets are investigated, and the results are compared with those of the unskewed machine. Furthermore, eddy current losses are computed by transient Finite Element Method (FEM) to estimate the ratio between eddy current, hysteresis, and ohmic losses.

II. ACTUATOR FORCE

Tubular linear synchronous motors belong to the linear drives. They convert electric energy into mechanical energy, in translational movement, and are constituted of fixed and mobile parts, i.e., stator and linor, respectively.

Compared to the planar form, radial attraction forces between stator and linor in tubular machines are compensated due to the rotational symmetry. Thus, the load on the bearings is reduced by several orders of magnitude and the bearings' lifetime is significantly increased. Furthermore, tubular linear motors provide a higher ratio of electromagnetic force per mass. This is due to the geometrical flux concentration in radial direction, and to the fact that the airgap area of the tubular machine is approximately twice the airgap area in a comparable planar design [3].

The drive system consists of a three-phase inverter bridge with six transistors and six freewheeling transistors. The conduction logic of each electronic switching device is performed according to the linor position, detected by a sensor. To increase the motor utilization, block current supply is applied to the coils.

A. Magnetic, Electric and Geometric Characteristics

The motor's magnetic, electric and geometric characteristics were obtained by means of classic electrical motor design rules. Firstly, the application demands were specified and according to them, some sizes were defined.

This work was supported by the State of São Paulo Research Foundations (FAPESP).

A. D. P. Juliani and D. P. Gonzaga are with Department of Electrical Engineering, São Paulo University, São Carlos, Brazil (e-mails: adpjuliani@usp.br and diogenes@sc.usp.br).

M. Leßmann and K. Hameyer are with Institute of Electrical Machines, RWTH Aachen University, Aachen, Germany (e-mails: marc.lessmann@iem.rwth-aachen.de and kay.hameyer@iem.rwth-aachen.de).

The magnetic circuit was analyzed in order to calculate the magnetic flux and the average electromagnetic force. Afterwards, the winding was determined [4, 5].

The designed motor is to be applied to the bioengineering area, especially to upper limb prostheses. Its dimensions are coherent with a man's forearm's size, as the machine will be allocated inside this space. The application demands and the features, such as the required electromagnetic force, the mechanical mechanism of finger and the minimum dislocation of the linor are according to [6].

The motor consists of a three-phase, massive iron stator with 18 coils per phase. The number of turns in each coil is 24 and the wire's diameter is equal to 0.373 mm. The linor is constituted by surface mounted, radial magnetized Neodymium Iron Boron (NdFeB) ring magnets, fixed on a massive back iron.

The 180° model of the motor is illustrated in Fig. 2 and its main characteristics are presented in table 1.

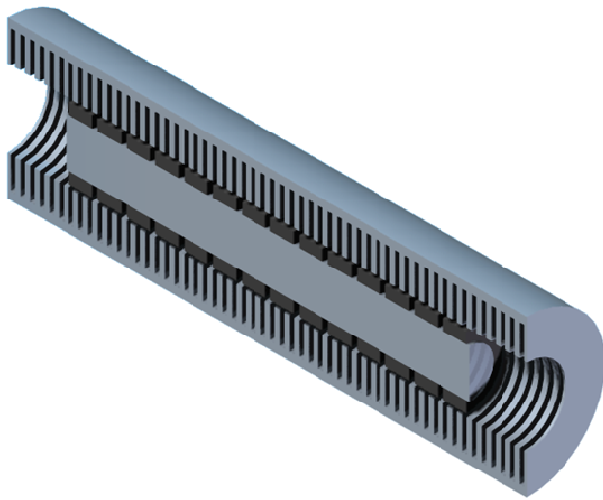


Fig. 2. 180° model of the motor with unskewed magnets.

Parameter	Unit	Value
Pole-Pitch	[m]	0.0051
Number of poles		14
Airgap length	[m]	0.0004
Outer stator radius	[m]	0.0139
Magnet Thickness	[m]	0.002
Axial filling factor of magnets	[%]	100
Remanent Induction of Magnets at 20°C	[T]	1.4
Rated Velocity	[m/s]	0.02
Number of coils per phase		18
Turns per stator slot		24
Wire diameter	[m]	0.000373
Rated current	[A]	7.69
Rated Electromagnetic Force	[N]	16.5

B. Investigated Skewing Methods

The tubular linear synchronous motor is responsible for actuating a single finger in an upper limb prosthesis. The main advantage of this type of motor is the absence of mechanical adaptation to produce the linear movement. This feature eliminates sounds that could bother the patient (such as the ones produced by the gears) and decreases the need of maintenance.

In this type of application, the ideal electromagnetic force should be constant, i.e. independent from linor position, due to the required accuracy. Nevertheless, it has oscillations that are usually caused by the cogging effect and pulsation of supply.

Firstly, this paper analyses the cogging force of the designed motor with unskewed magnets, illustrated in Fig. 3. Next, small permanent magnet blocks are arranged parallel to each other (i.e. all axially oriented), following two helical paths with opposite screw directions, starting at the same point and meeting again diametric at the opposite side of the cylinder (Fig. 4). In the last part, individual magnet pieces are cut in one piece out of a hollow cylinder of magnetic material with two parallel oblique planes (i.e. not parallel with the axis of the cylinder), shown in Fig. 5. For each skewing method, different variations of axial magnet filling factor are investigated, i.e. the ratio of axial vs. maximum axial magnet length when magnets are axial aligned.



Fig. 3. Unskewed magnets on the linor surface of one pole pair: a) Dimetric view; b) Front view.



Fig. 4. Skewed magnets on the linor surface of one pole pair: a) Dimetric view; b) Front view.



Fig. 5. Plane skewed magnets on the linor surface of one pole pair: a) Dimetric view; b) Front view.

C. Results

Both electromagnetic and cogging forces were calculated by means of the 3-dimensional Finite Element Method (FEM), in order to take the skewing effects into account.

The results were obtained by the iMOOSE.tsa3d transient solver, an extension of the iMOOSE [7] numerical environment.

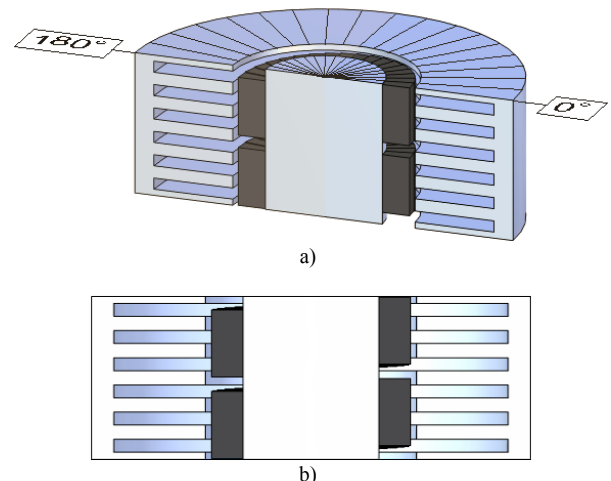


Fig. 6. One pole pair of the motor with skewed magnets: a) Dimetric view; b) Front view.

The multi-slice method [5] was used to avoid the calculation with the 180° motor model, thus, the computational time was reduced. This method is based on dividing the 180° model into several slices, here 10°, to compose the entire motor, as depicted in Fig. 6. The final result is obtained by the superposition of the computational steps [5].

First, the optimum commutation angle, delivering the highest torque, was determined with the unskewed model.

To obtain the optimum commutation angle, the current feed of the coils was varied in commutation steps of 10°, according to the linor, as illustrated in Fig. 7. Thus, the optimum commutation angle amounts to 0°.

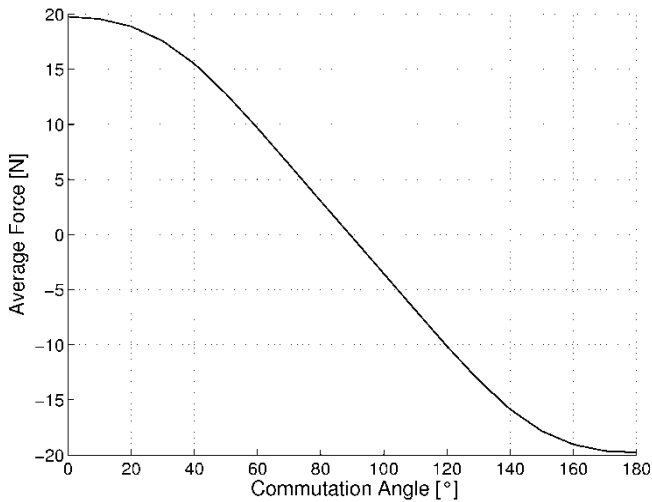


Fig. 7. Average force versus commutation angle.

Fig. 8 shows the resulting actuator force as the sum of cogging force and propulsion force for the unskewed model exemplary for a non-optimum commutation angle equal to 40°. Commutation of the stator currents is performed at an electrical angle of axial displacement of 20° and 80°, observed by the steps in propulsion force. Thereby, average actuator force is reduced to 15.5 N.

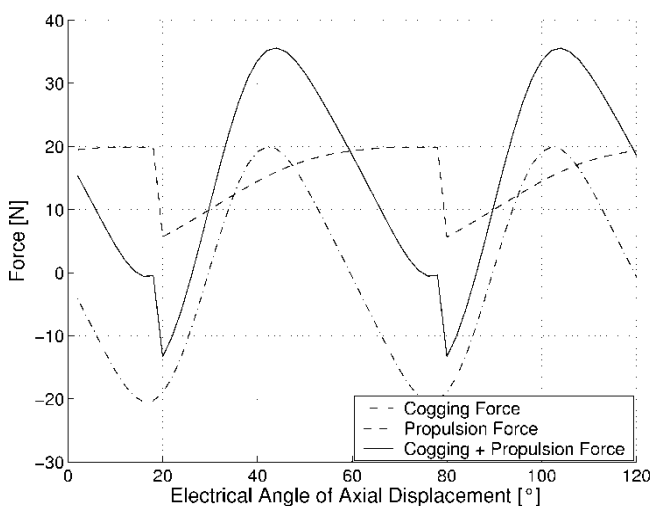


Fig. 8. Cogging force, propulsion force, and resulting actuator force for commutation angle equal to 40°.

Fig. 9 depicts the forces under same operation condition but at optimum commutation angle of 0°. Here, commutation is performed at an electrical angle of axial displacement of 0°, 60°, and 120°.

During commutation, no step in propulsion force is observed, resulting in a maximum average actuator force of 19.4 N and minimum ripple in propulsion force of 0.63 N, caused by end effects of the permanent magnets, providing a not ideal rectangular air gap field. Although the required rated electromagnetic force of 16.5 N is achieved, peak value of cogging force is equal to average actuator force. Thus, the demand for constant actuator force under nominal operation is not achieved so far.

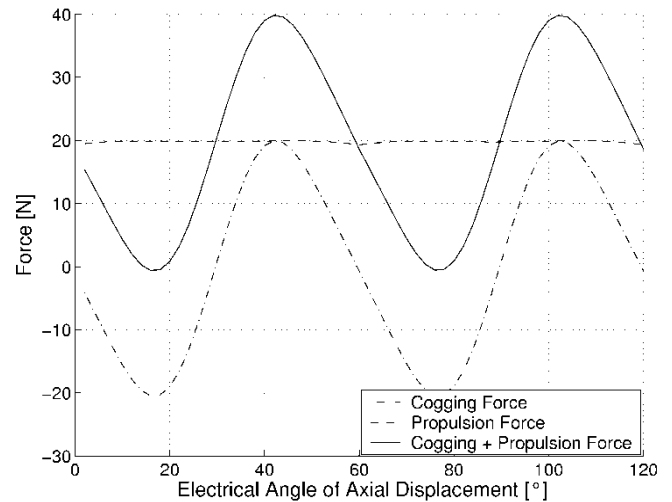


Fig. 9. Cogging force, propulsion force and resulting actuator force at optimum commutation angle of 0°.

In conventional rotary machines, skewing of the rotor magnets for one stator tooth pitch is usual to reduce the cogging torque [4]. This method, in the following called skewed method, is applied to the tubular linear motor, as depicted in Fig. 4. As shown in Fig. 10, force ripple is reduced from 41.6 N of the unskewed model to 2.0 N of the skewed model. Hence, the ratio of force ripple to average force is improved from 2.14 to 0.11. Average force reduction, caused by the skewing effects, amounts to 3.5 %.

Problematical in this design of the linor is the mechanical feasibility of the magnets' skewing because of the very small dimensions of the magnet pieces of 2mm x 5.1mm x 0.75mm. A total of 504 magnet pieces is required for linor assembly, making feasibility quiet impossible.

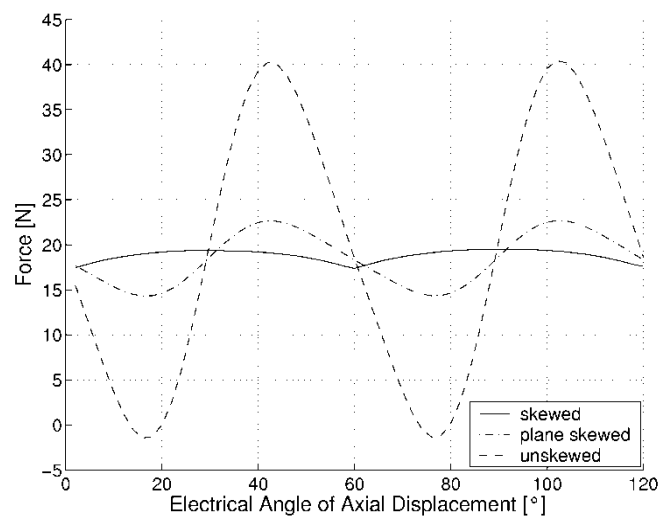


Fig. 10. Comparison of resulting actuator forces for different skewing methods.

To reduce manufacturing complexity, the skewing method, presented above in Fig. 5, is investigated alternatively. The 36 magnets, arranged in the skewed circle (Fig. 4), are exchanged by an adequate magnet cylinder, cut by laser of a magnet ring (Fig. 5).

This method is called plane skewed method below. Computational results are depicted in Fig. 10. Force ripple is reduced from 41.6 N of unskewed to 8.32 N of plane skewed method. Thus, the ratio of force ripple to average force is improved from 2.14 to 0.45. Average force reduction, caused by the skewing effects, amounts to 4.5 %.

The comparison between the skewed and plane skewed method yields in a factor four better results of ripple to average force ratio for the skewed method. Average force reduction compared to unskewed model is marginal less with the skewed model. Hence, the skewed method should be preferred if feasibility permits.

Another possibility to reduce the force ripple, caused by the cogging effects, is the design of the linor. Wang et al. [8] describe a strong dependency between the cogging force and the axial filling factor of magnets. Their work predicts a minimum in cogging force at a filling factor of 80 %, independent on other geometrical dimensions. Results of FE computation, as depicted in Fig. 11, observe the minimum at a filling factor of about 76 %, which is in good agreement with Wang's analysis. Force ripple is reduced to 3.9 N, only about half of the force ripple of plane skewed method. Thus, ratio of force ripple to average force amounts to 0.21.

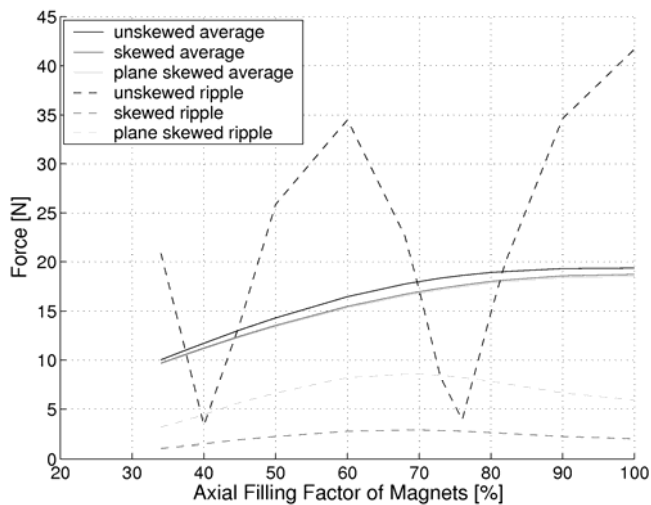


Fig. 11. Ripple and average actuator force for different skewing methods as function of axial filling factor of magnets.

However, FE results yield a strong gradient in force ripple besides the minimum. Thus, lowest manufacturing tolerances already increase force ripple for several orders of magnitude. A deviation on axial filling factor of 4 % in the minimum, i.e. 155 μm in axial magnet length, already causes a factor three in force ripple rise. Reduction of average force due to decrease in permanent magnetic material amounts to negligible 3.8 %.

For skewed and plane skewed method, the reduction of magnets' axial filling factor has negative effect to the ratio of force ripple to average actuator force. As force ripple is increasing with reduction of axial filling factor of magnets, average force is decreasing. Thus, best ratio of force ripple to average force is achieved at 100 % axial magnet filling factor.

There is no significant difference in the actuator's average force between the skewed and the plane skewed method, but the cogging force of the second situation is more than three times as high as the first one. The reason for this dissimilarity is that, different from the skewed model, the plane skewed magnets do not have a constant displacement gradient in the axial direction.

III. LOSSES

All kind of losses, especially in implants, are critical in bioengineering, increasing temperature of the surrounding tissue. Surface temperatures above 42 $^{\circ}\text{C}$ increase the risk of hemolysis and thrombogenicity [2]. Hence, all kind of losses have to be investigated and reduced to a minimum.

Three dominant sources of losses occur in permanent magnet excited tubular linear motors, i. e. the ohmic losses in the stator coils, the eddy current losses in all electric conducting parts as well as the hysteresis losses in ferromagnetic materials.

The ohmic losses in the stator coils amounts to 6,54 W at rated torque. To minimize them by increasing the magnetic flux, NdFeB permanent magnets with highest magnetic energy are chosen. Nevertheless, this magnetic material is electrically conductive, permitting the induction of eddy currents. The magnets, fixed on the linor surface, are affected by the magnetic field of the stator. Time dependent gradients in magnetic flux (caused by the stator slots, the movement of the linor, and the current commutation) induce eddy currents in the magnets, as well as in the back iron of the stator and linor.

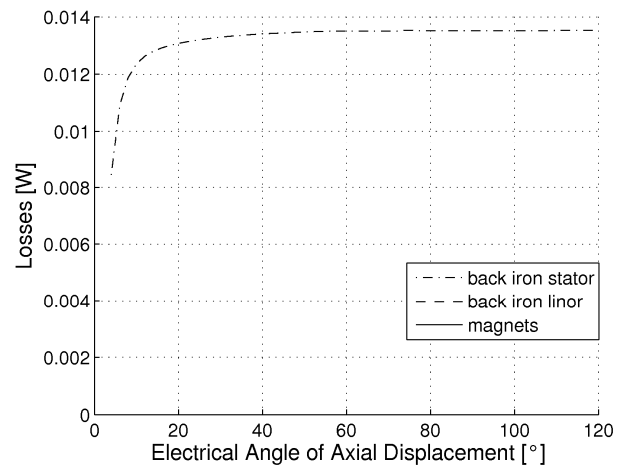


Fig. 12. Time dependent characteristic of the induced eddy currents into the magnets and the back iron of stator and linor at rated speed and no-load.

Fig. 12 depicts the induced eddy current losses into the magnets and the back iron of stator and linor, computed with the transient solver iMOOSE.tsa3d [7]. Computation was performed at the rated velocity of 20 mm/s at no-load. Thus, commutation losses do not occur. Electrical conductivities were assumed to $1 \times 10^6 \text{ 1}/\Omega\text{m}$ for back iron and $0.71 \times 10^6 \text{ 1}/\Omega\text{m}$ for permanent magnet material. Until an electrical angle of axial displacement of 40 $^{\circ}$, transient effects decay. In stationary operation, the induced eddy currents into the stator back iron amounts to 13.5 mW. The eddy currents induced into the linor back iron and the magnets are congruent with the x-axis and negligible accordingly. Fig. 13 illustrates the distribution of the eddy current density in this operation point.

In the region of the stator teeth next to the linor, eddy current density achieves the maximum value due to the minimum ohmic resistance of the electric conductive material in this region.

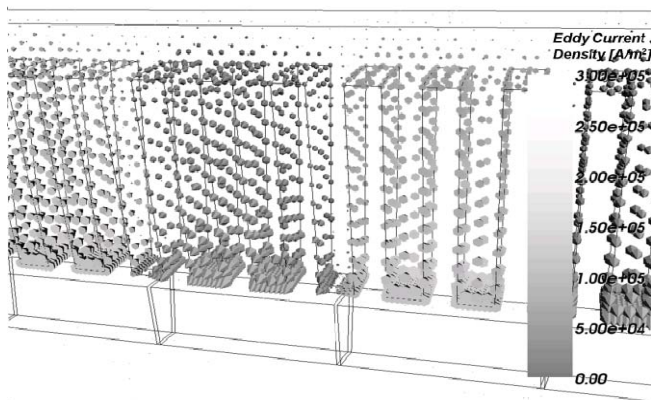


Fig. 13. Distribution of the induced eddy currents into the magnets and the back iron of stator and linor at rated speed and no-load.

Due to the block current feed, commutation losses occur additionally as depicted in Fig. 14 at rated force for one commutation step. According to the induced eddy currents at no-load, only the losses in the stator back iron are significant as the zoom depicts. Fig. 15 b) and Fig. 16 illustrate the distribution of the eddy currents during commutation at rated force and velocity. The commutated coils can be clearly identified by the high eddy current density. Additionally, the small amount of eddy currents induced into the linor back iron during commutation can be recognized.

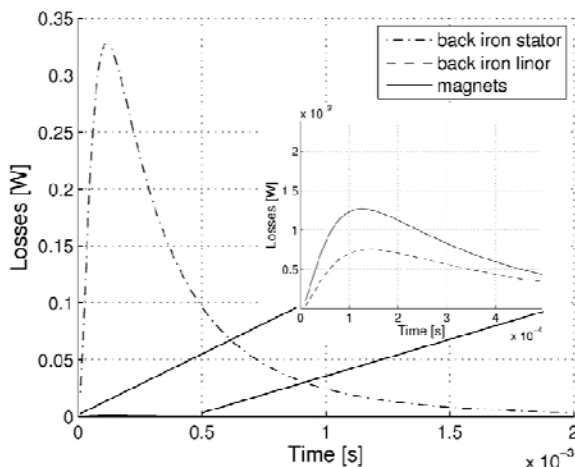


Fig. 14. Commutation losses for one commutation step at block current fed and rated force.

Fig. 17 illustrates the overall amount of eddy current losses at different linor speeds. The zoom depicts the characteristic of eddy current losses as a function of linor displacement during commutation. The width of the curves is proportional to the linor speed whereas the amplitude only depends on the square of the amplitude of the commutated currents.

After transient effects of commutation have decayed, the remaining eddy current losses are proportional to the square of linor's speed. Due to the low rated speed of the linor according to about 2 Hz electrically, the amplitude of these losses only amounts to less than 5 % of commutation losses. Nevertheless, commutation losses decay quickly. Thus, total average eddy current losses amount to 14.2 mW at rated speed and torque. Hence, eddy current losses are negligible compared to the ohmic losses in the stator coils of 6.54 W at rated force.

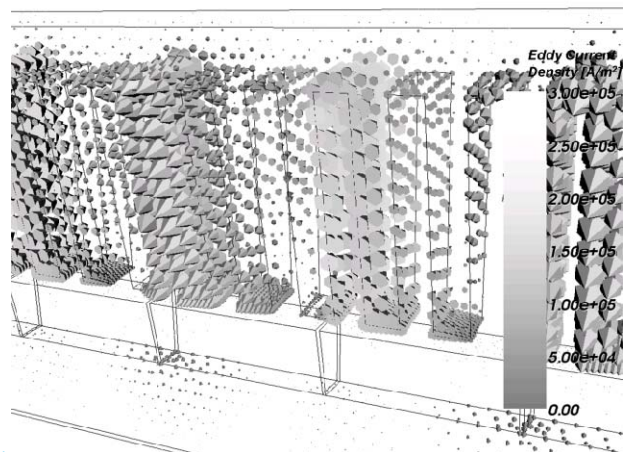


Fig. 16. Distribution of eddy currents during commutation at rated force.

In conventional rotary machines, these eddy current losses are reduced by interruption of the eddy current paths, i.e. replacement of massive structural components by laminated sheets or soft magnetic composites (SMC). This approach is not constructionally applicable to the tubular linear motors. The lamination has to be performed in radial direction parallel to the centerline of the linor, whereas SMC does not provide the required mechanical strength.

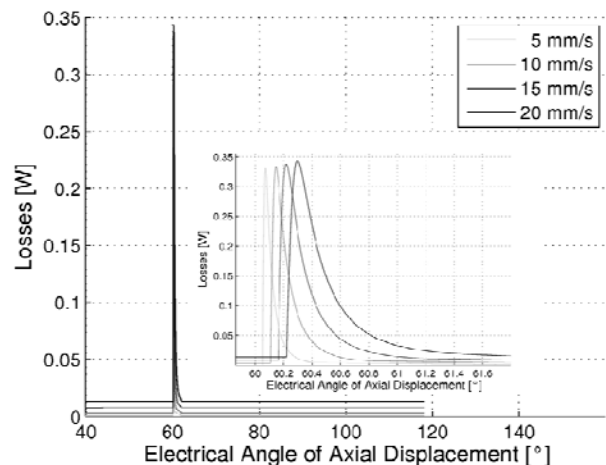


Fig. 17. Overall amount of eddy current losses. The zoom depicts the commutation losses as commutation is performed at 60°.

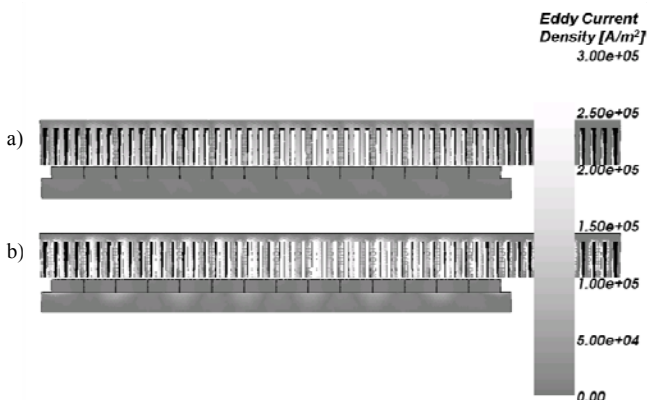


Fig. 15. Distribution of eddy current density during commutation at rated force and velocity a) after commutation effects decayed and b) during commutation.

At least the hysteresis losses in all ferromagnetic components have been investigated. As observed in the eddy current computations, induced eddy currents into the linor are negligible due to the quasi static magnetic field in the linor. Hence, significant hysteresis losses only occur in the back iron of stator. Investigations of hysteresis losses in iron have been performed in advance by measurements and FE computations. At sinusoidal, homogeneous magnetic excitation of 50 Hz at an amplitude of 1.5 T, hysteresis losses density amounts to 2 W/kg. Based on the linear dependency between hysteresis losses and frequency, hysteresis losses in stator back iron, which weight amounts to 0.214 kg, have been estimated to 17.1 mW at a field frequency of 2 Hz and 1.5 T amplitude. Thus, hysteresis losses are in the same order of magnitude as eddy current losses and negligible compared to the ohmic losses.

IV. CONCLUSIONS

This paper analyzed the cogging force of a tubular linear synchronous motor designed to be applied to an upper limb prostheses.

The designed linear motor with unskewed magnets and a permanent magnet filling factor of 100 % features a high ratio of force ripple to average force of 2.14. Thus, the amplitude of cogging force is of the same order of magnitude as the rated force. A solution proposed to decrease the cogging force was to apply the effects of skewing on magnets. First, the ideal skewed model with a constant gradient in permanent magnet axial displacement presented a reduced ratio of force ripple to average force of 0.11. To assure the mechanical feasibility a simplification in the construction of the linor was performed by cutting a hollow cylinder of magnetic material with two parallel oblique planes. In this case, the ratio of force ripple to average force is four times higher and amounts to 0.45.

To generally avoid the mechanical feasibility conjunct with skewed magnets, the variation of the axial permanent magnet filling factor with unskewed magnets was investigated. Minimum ratio of force ripple to average force of 0.21 is achieved at an axial permanent magnet filling factor of 76 %. However, FE results yielded a strong gradient in force ripple besides the minimum. Thus, lowest manufacturing tolerances already increase force ripple for several orders of magnitude.

In summary, the plane skewed linor achieves the requirements best, taking mechanical feasibility into account.

Due to the increased risk of blood damage in bioengineering at temperatures above 42 °C, all kinds of losses in the linear motor were computed. Although the back iron of the stator is massive, the induced eddy currents into the stator by the movement of the linor and the current commutation are negligible compared to the ohmic losses in the stator coils, which amount to 6.54 W. Causes are the low electric frequencies of 2 Hz at rated linor speed. Due to the quasi static field in the linor, eddy currents induced in the back iron of the linor and the permanent magnets only amounts to several μ W. Thus, specific ohmic losses per stator surface amounts to only 82 mW/cm² at rated force and can be conducted to the surrounding tissue without exceeding temperature limitations of 42 °C.

Hysteresis losses are in the same order of magnitude as the eddy current losses, as estimations have shown. Thus, only ohmic losses are relevant for thermal aspects.

At the moment, prototypes are under construction in order to compare the simulation with experimental results. Additionally, thermal analysis will be done to verify the temperature in the actuator.

V. REFERENCES

- [1] J. F. Gieras, and M. Wing, *Permanent Magnet Motor Technology – Design and Applications*, 2nd ed. New York: Marcel Dekker Inc, 2002, p. 1.
- [2] T. Finocchiaro, S. Heinke, M. Behbahani, M. Leßmann, M. Laumen, U. Steinseifer, T. Schmitz-Rode, S. Leonhardt, M. Behr, and K. Hameyer, “Methods of design, simulation, and control for the development of new VAD/TAH concepts,” *Biomedizinische Technik*, special issue: Smart Life Support, vol. 54, no. 5, pp. 269-281, 2009.
- [3] A. W. Zyl, C. G. Jeans, R. J. Cruise, and C. F. Landy, “Comparison of force to weight ratios between a single-sided linear synchronous motor and a tubular linear synchronous motor,” in *Proc. 1999 IEEE International Electric Machines and Drives Conf.*, pp. 571-573.
- [4] G. Müller, K. Vogt, and B. Ponick, *Berechnung elektrischer Maschinen*. Weinheim: WILEY-VCH Verlag, 2008.
- [5] B. Schmülling, M. Leßmann, B. Riemer, and K. Hameyer, “The multi-slice method for the design of a tubular linear motor with a skewed reaction rail,” *COMPEL*, vol. 29, no. 5, accepted for publication, Emerald Group Publishing Limited, 2010.
- [6] L. Zollo, S. Roccella, E. Guglielmelli, M. C. Carrozza, and P. Dario, “Biomechatronic design and control of an anthropomorphic artificial hand for prosthetic and robotic applications,” *IEEE/ASME Trans. on Mechatronics*, vol. 12, no 4, pp. 418-429, 2007.
- [7] D. van Riesen, C. Monzel, C. Kaehler, C. Schlensock, and G. Henneberger, “iMOOSE – an open-source environment for finite-element calculations,” *IEEE Trans. on Magnetics*, vol. 40, no. 2, pp. 1390-1393, 2004.
- [8] WANG, J.; JEWELL, G. W.; HOWE, D., “Design Optimization and Comparison of Tubular Permanent Magnet Machine Topologies,” in *IEE Proc. 2001 Electr. Power Appl*, vol. 148, no 5, pp. 456-464.

VI. BIOGRAPHIES

Aline Durrer Patelli Juliani (born in 1981) obtained a degree in electrical engineering from São Paulo State University, Bauru, Brazil, in 2005. She received the M.S. degree in electrical engineering from São Paulo University, in São Carlos, Brazil. She is currently a PhD student at the same University. Her research interests include electrical machines, motor drives and motion control, finite element analysis, and prosthetic hands.

Marc Leßman (born in 1977) graduated in electrical engineering at the RWTH Aachen University, Germany, in 2004. Currently he is PhD student at the Institute of Electrical Machines of RWTH Aachen University. His research interests are high speed machines, linear drives, electromagnetic levitation techniques, and the development of life support systems such as total artificial hearts and ventricular assist devices.

Diógenes Pereira Gonzaga (born in 1948) received his Engineering Degree in 1975 from Engineering School of São Carlos, São Paulo University, Brazil and his Doctorate degree in Engineering in 1993 from the State University of Campinas, Brazil. After graduation, he worked at the Heavy Equipment Department of General Electric of Brazil, Campinas. Since 1978 he has been working in the Dept of Electrical Engineering at the São Paulo University, Engineering School of São Carlos, Brazil, where he is currently an Associate Professor. His main areas of interest are electric and magnetic circuits, electromechanical energy conversion, and modeling and simulation of electrical machines.

Kay Hameyer (born in 1958) received his PhD from the University of Technology Berlin, Germany, 1992. From 1986 to 1988 he worked with the Robert Bosch GmbH in Stuttgart, Germany, as a design engineer for permanent magnet servo motors. In 1988 he became a member of the staff at the University of Technology Berlin, Germany. Until 2004, he was professor of numerical field computation and electrical machines with the K.U. Leuven and a senior researcher with the FWO-V in Belgium, teaching CAD in electrical engineering and electrical machines. Currently, he is Head of the Institute of Electrical Machines of RWTH Aachen University, Germany. His research interests are numerical field computation, the design of electrical machines, in particular permanent magnet excited machines, induction machines and numerical optimisation strategies. Prof. Hameyer is a member of the International Compumag Society and senior member of the IEEE.